Mechanism and kinetics of acetyl-lysine binding to bromodomains

SUPPLEMENTARY INFORMATION

A. Magno[a‡], S. Steiner[a‡], and A. Caflisch[a*]

[a]Department of Biochemistry
University of Zürich, Winterthurerstrasse 190
CH-8057 Zürich, Switzerland
Phone: (+41 44) 635 55 21, FAX: (+41 44) 635 68 62
email: caflisch@bioc.uzh.ch

*Corresponding author

‡ These authors contributed equally to this work

keywords: molecular dynamics, post-translational modifications, histones, epigenetic marks, acetylated lysine, cut-based free energy profile

July 4, 2013

Bromodomain (PDB code)	Ligand	Force Field	Starting structure	No. of runs	Total sampling [μs]
TAF1(2) (3UV4)	Kac	CHARMM	Unbound, Asn1604 χ_2 up	12	6
TAF1(2) (3UV4)	Kac	CHARMM	Unbound, Asn1604 χ_2 down	12	6
TAF1(2)	Kac	AMBER	P-binding from CHARMM	2	2
TAF1(2)	Kac	AMBER	N-binding from CHARMM	2	2
BRD4(1) (3UVW)	Tetrapeptide	CHARMM	X-Ray	2	2
CREBBP (3P1C)	Tetrapeptide	CHARMM	Overlap on 3UVW	2	2
BRD4(1)	Tetrapeptide	AMBER	from CHARMM run	2	2
CREBBP	Tetrapeptide	AMBER	from CHARMM run	2	2

Table S1: Simulations performed.

Transitions from \ to	**Unbound**	**P-binding**	**N-binding DOWN**	**N-binding UP**	**P/N-Intermediate**
Unbound	-	1	2	12	5
P-binding	2	-	119	10	310
N-binding DOWN	2	118	-	18	4
N-binding UP	2	17	18	-	13
P/N-Intermediate	4	312	6	10	-

Table S2: The number of transitions between the different basins after splitting of the N-binding basin into two sub-basins characterized by different values of Asn1604 χ_2.

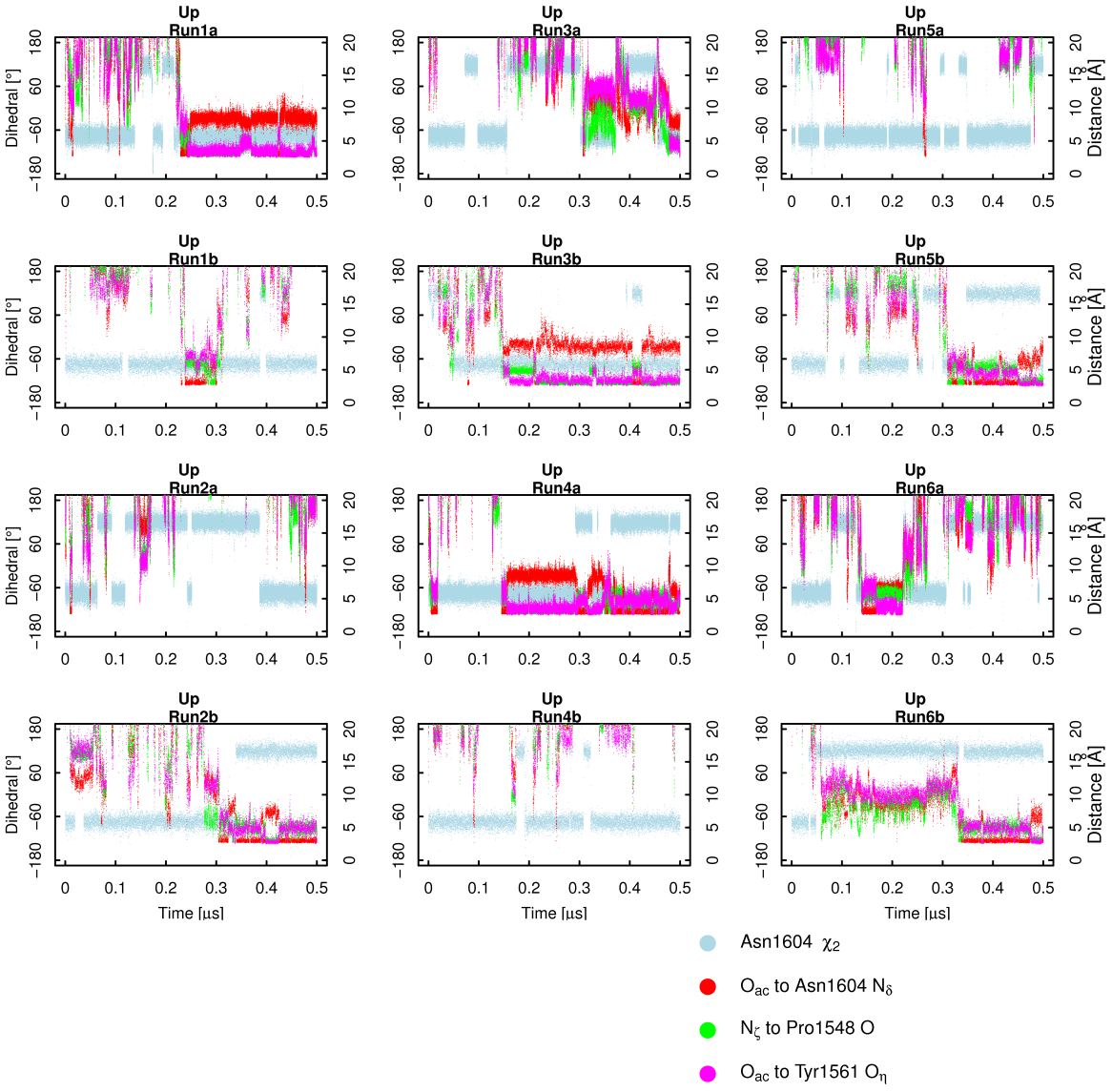

Figure S1: Time series of the interatomic distances between donor and acceptor atoms of three intermolecular key interactions (red, green, and magenta, y-axis on the right) together with the time series of the χ_2 dihedral angle of the conserved Asn1604 (cyan, y-axis on the left) for the 12 individual runs started with the N_δ atom of Asn1604 pointing towards the solvent (Up). The letters *a* and *b* distinguish two runs started from the same starting structure using different seeds.

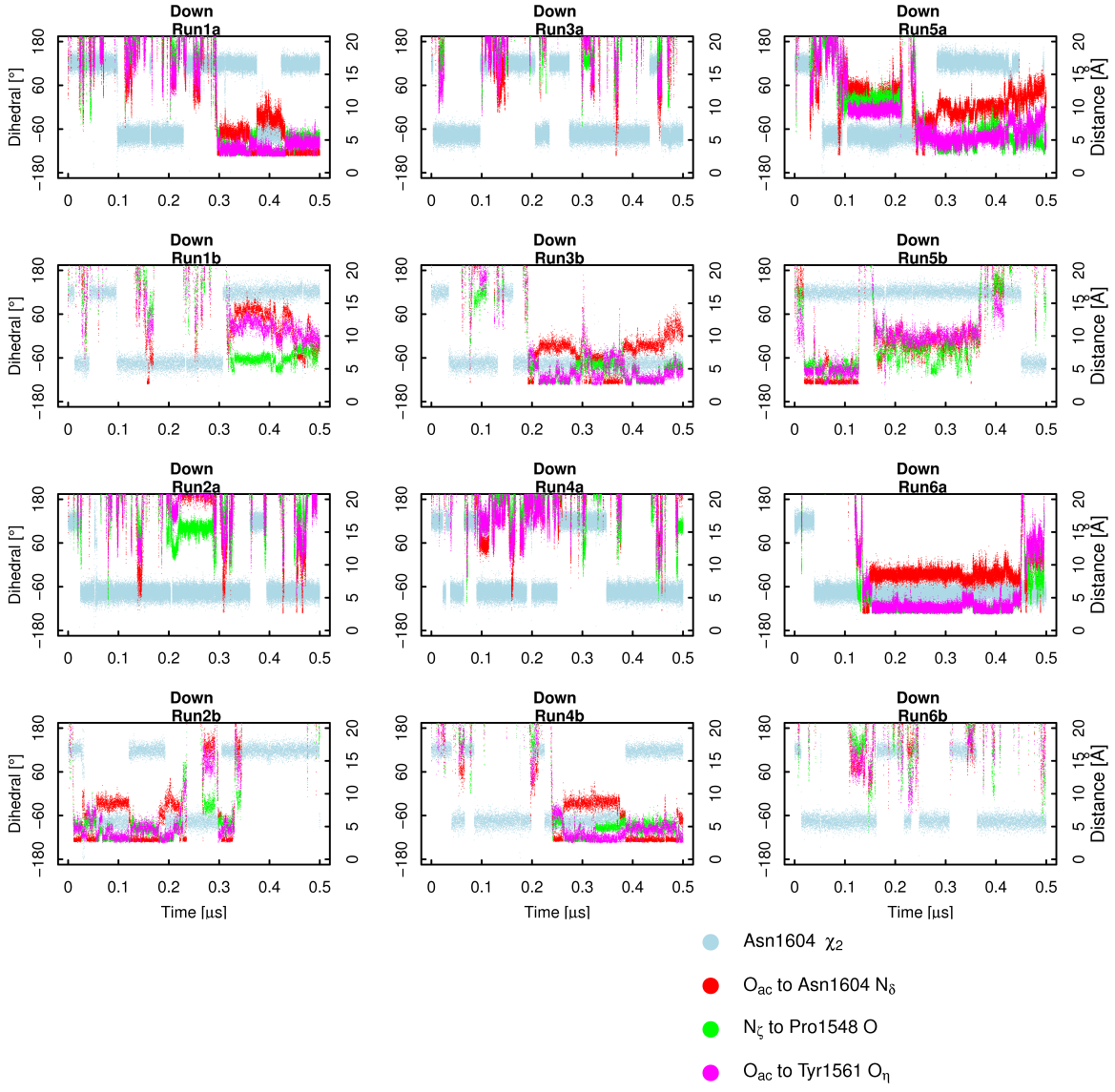

Figure S2: Same as in Figure S1 for the 12 individual runs started with the N_δ atom of Asn1604 pointing towards the binding site bottom (Down).

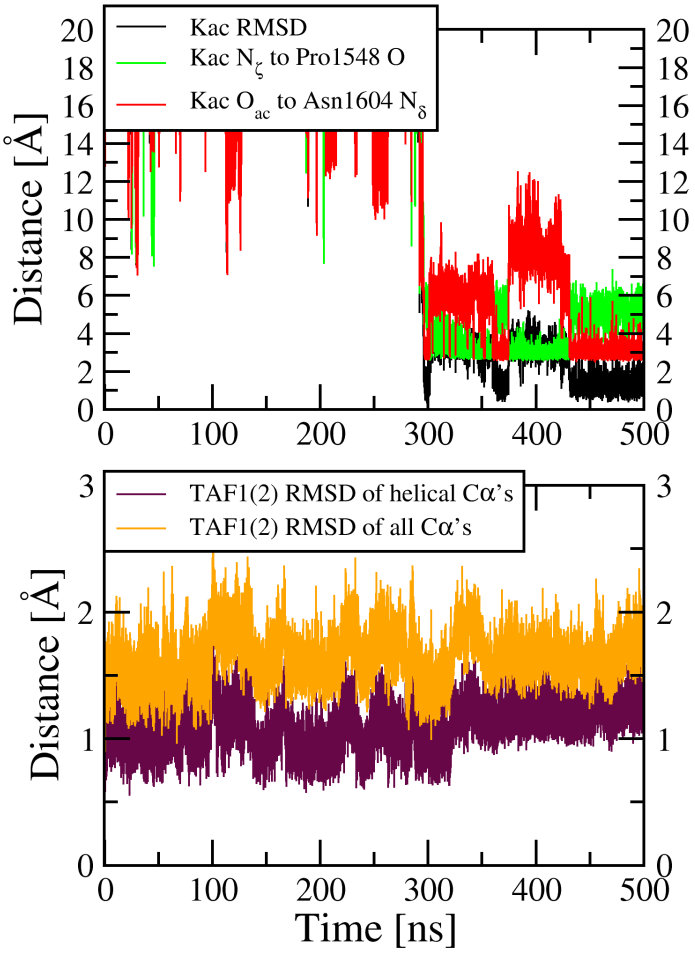

Figure S3: (Top) Time series of the RMSD from the X-ray structure (black) together with the distances that characterize the hydrogen bond observed in the crystal structures (red) and the hydrogen bond of the more buried binding mode revealed by the present MD study (green). The RMSD of the Kac side chain atoms was calculated upon optimal overlap of the C_α atoms in the four helices. The reference structure for the RMSD calculation was the crystal structure of CREBBP in complex with Kac (PDB code 3P1C) as there is no crystal structure of TAF1(2) with Kac or a histone tail peptide. (Bottom) Time series of the RMSD from the equilibrated conformation of TAF1(2) C_α atoms (orange) and C_α atoms in helices only (maroon). These time series show that upon Kac binding the bromodomain structure becomes slightly less flexible but does not undergo any relevant conformational change.

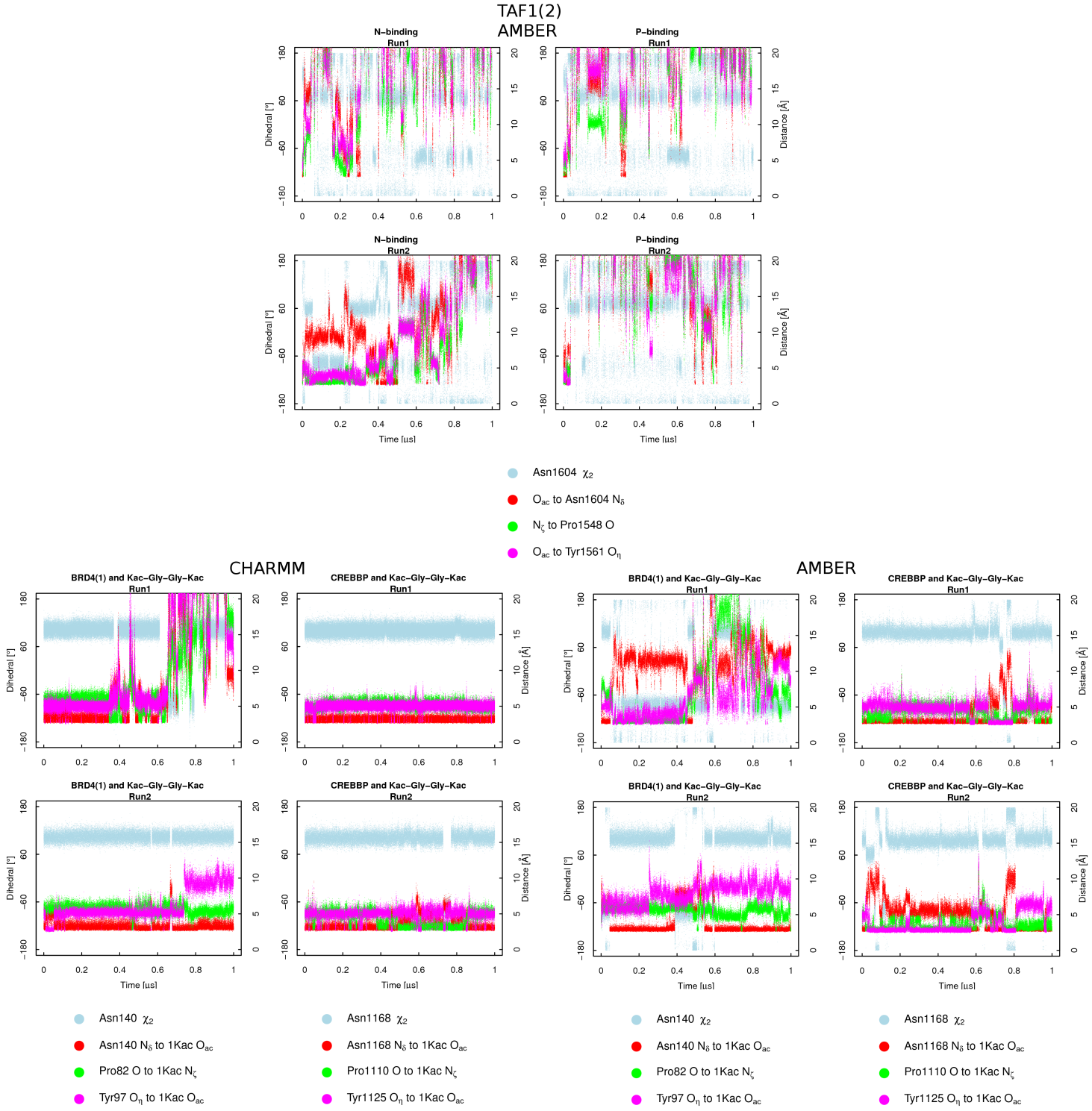

Figure S4: Control simulations with the AMBER force field and/or the tetrapeptide Kac-Gly-Gly-Kac. (Top) Time series of the interatomic distances between donor and acceptor atoms of three intermolecular key interactions (red, green, and magenta, y-axis on the right) together with the time series of the χ_2 dihedral angle of the conserved Asn in the binding site (cyan, y-axis on the left) for the control simulations of TAF1(2) and Kac with AMBER force field. (Bottom) Time series of interatomic distances between the N-terminal Kac of the tetrapeptide Kac-Gly-Gly-Kac and BRD4(1) or CREBBP for the simulations with the CHARMM (bottom left) or AMBER (bottom right) force field.

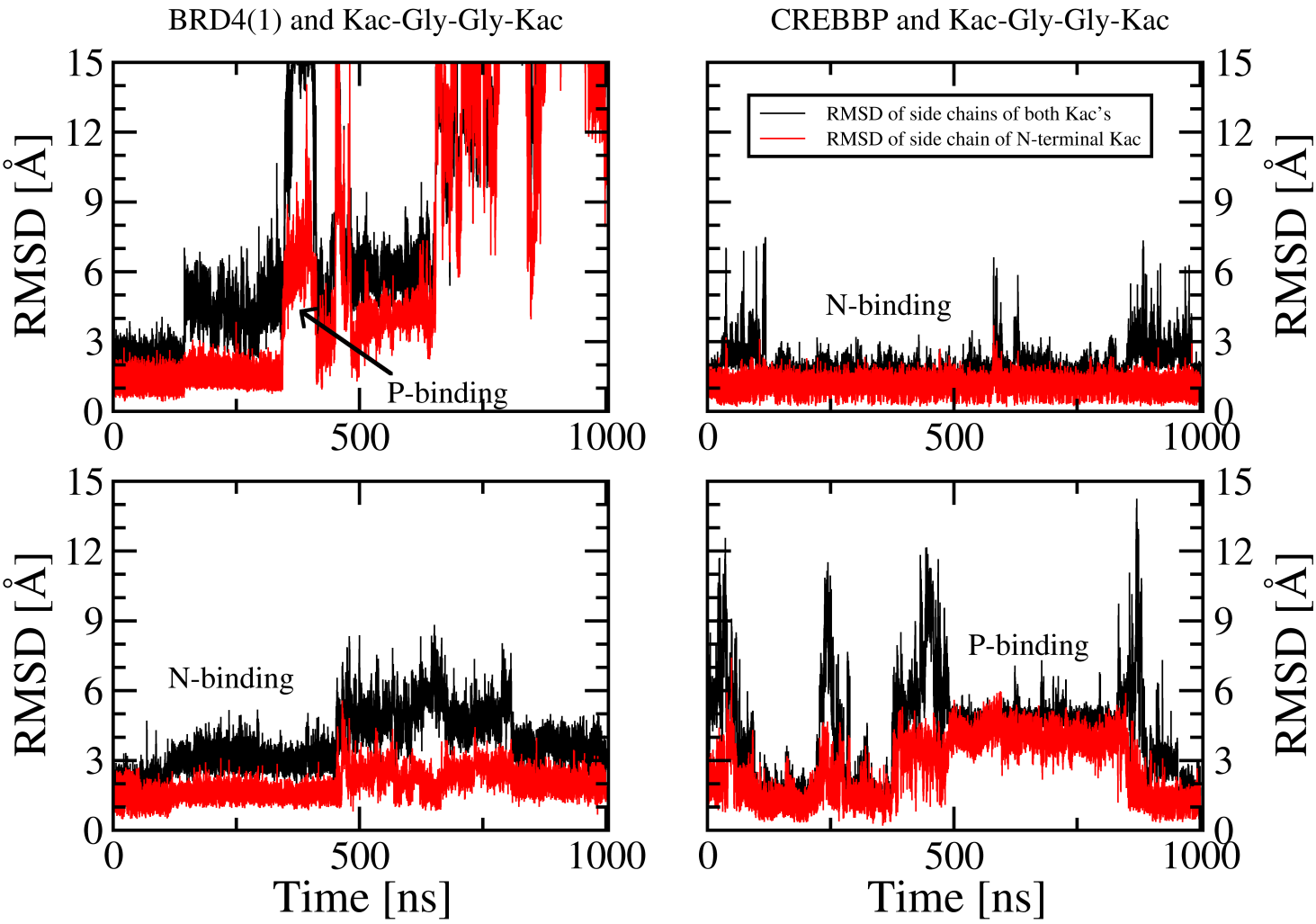

Figure S5: Control simulations with the CHARMM force field and the tetrapeptide Kac-Gly-Gly-Kac. Time series of the RMSD of the side chain atoms of the two Kac's (black) and only the N-terminal Kac (red) for two independent runs each with BRD4(1) (left) and CREBBP (right). The RMSD was calculated upon optimal overlap of the C_α atoms in the four helices of the bromodomain. The reference structure for the RMSD calculation was the crystal structure of BRD4(1) in the complex with Kac-Gly-Gly-Kac from the histone 4 peptide H4K5acK8ac (PDB code 3UVW).

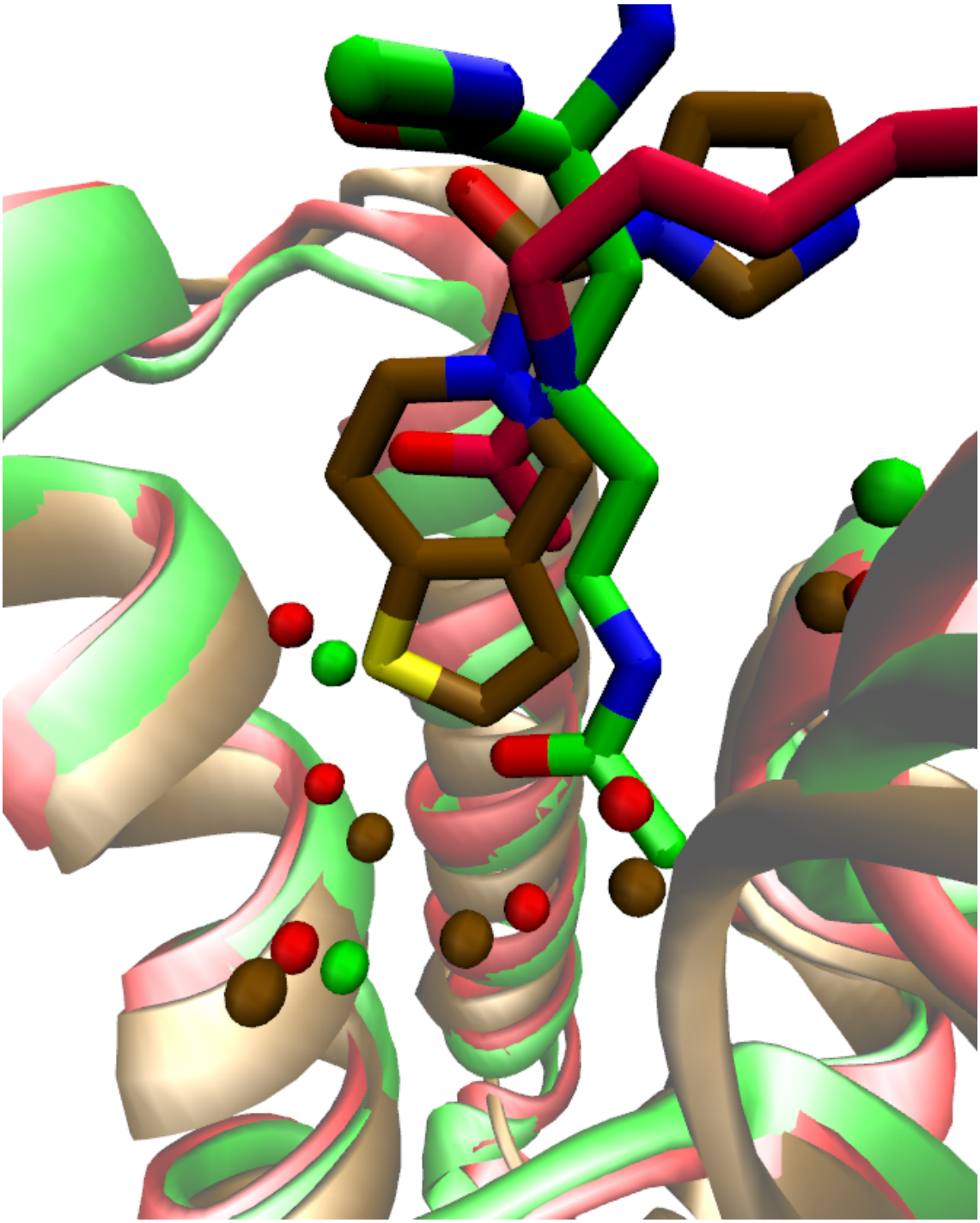

Figure S6: Small molecule inhibitors of brodomains can penetrate deeply into the acetyl-lysine binding pocket similarly to the P-binding mode of Kac observed in the MD simulations. Representative snapshots of acetyl-lysine in the P-binding mode (green) and N-binding mode (red) are structurally aligned, using only the C_α atoms of the bromodomain helices, to the crystal structure of BRD4(1) in complex with a recently published inhibitor (brown, PDB code 4HXK). The bromodomain backbone, Kac/inhibitor, and structured water molecules are shown as ribbons, sticks and spheres, respectively.

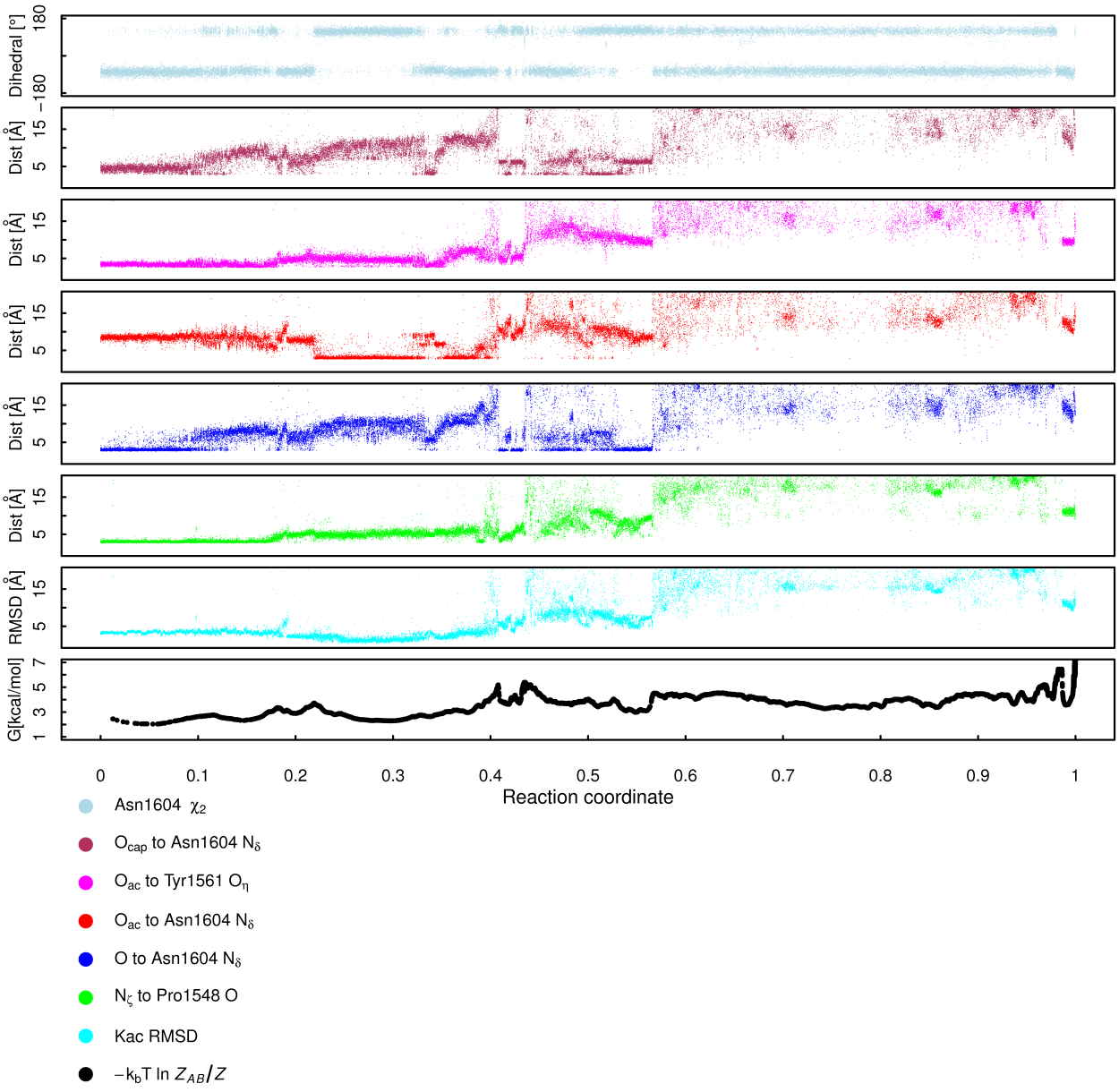

Figure S7: Geometric annotation and cFEP (bottom panel) with the P-binding mode representative as reference node. The RMSD (second panel from the bottom) of the Kac atoms with respect to the X-ray structure reported in 3P1C was calculated after overlap of the TAF1(2) C_α atoms to the corresponding atoms of CREBBP in 3P1C.

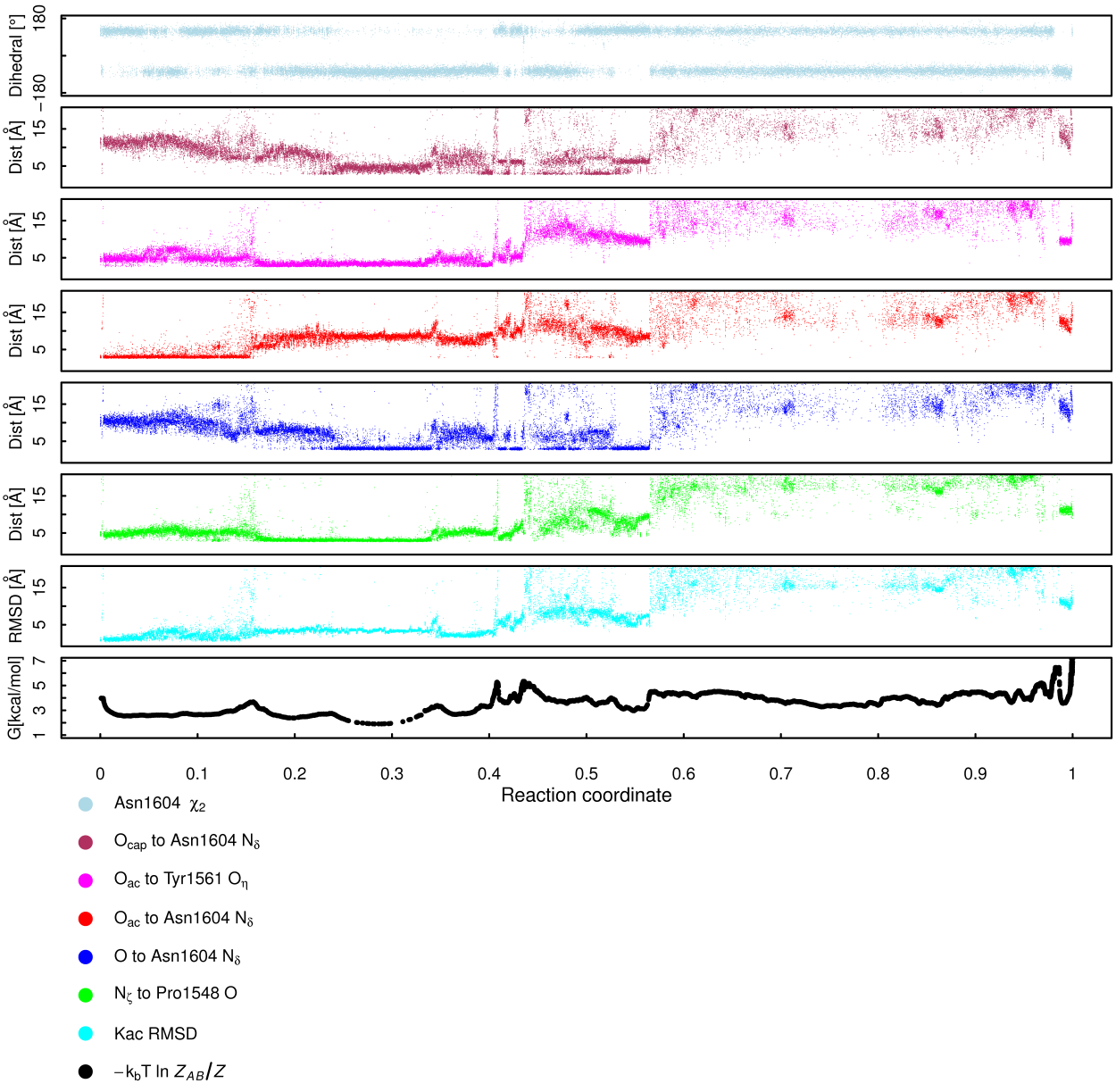

Figure S8: Geometric annotation and cFEP (bottom panel) with the N-binding mode representative as reference node. For further details see legend of Figure S7.

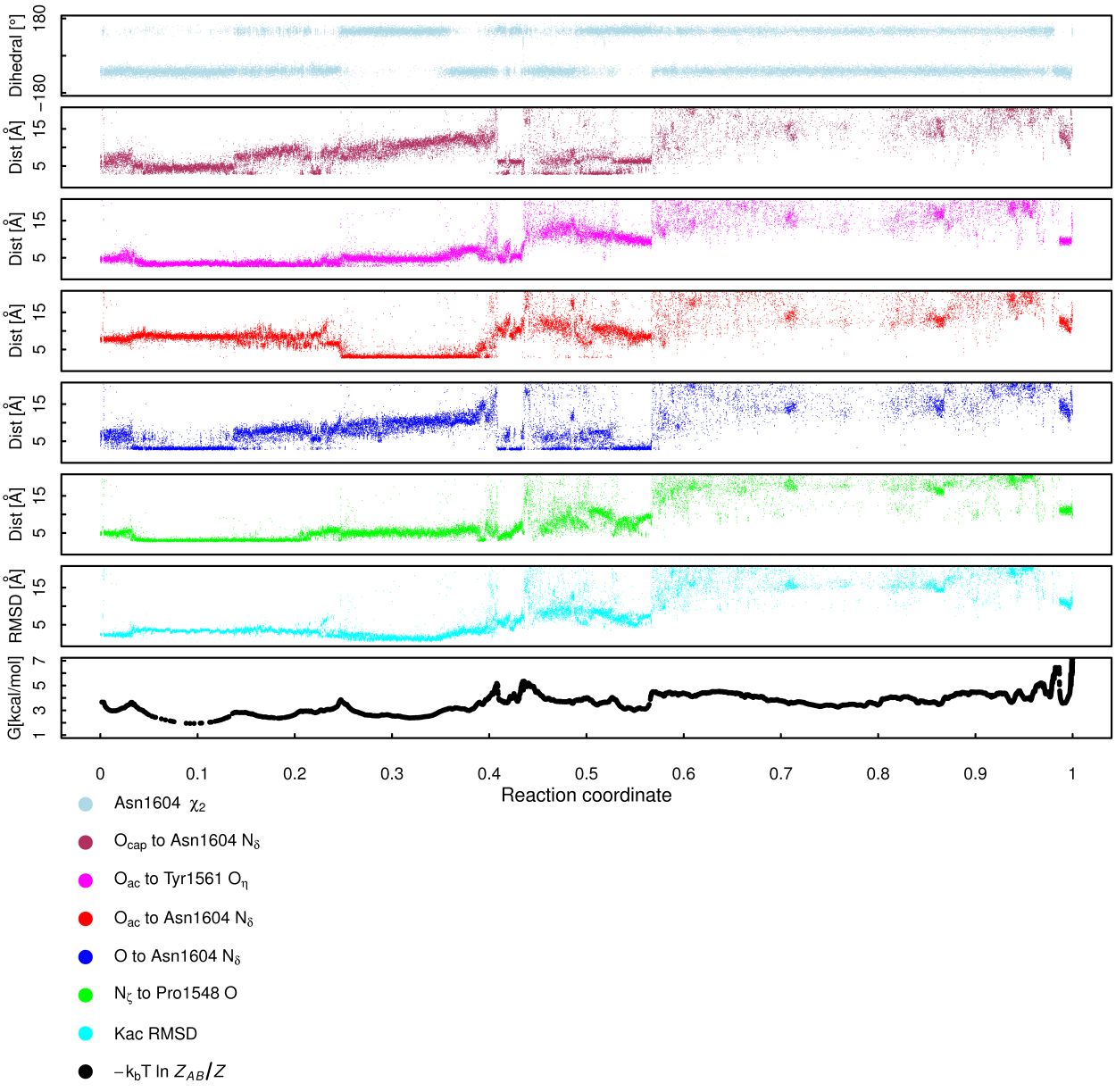

Figure S9: Geometric annotation and cFEP (bottom panel) with the P/N-Intermediate representative as reference node. For further details see legend of Figure S7.

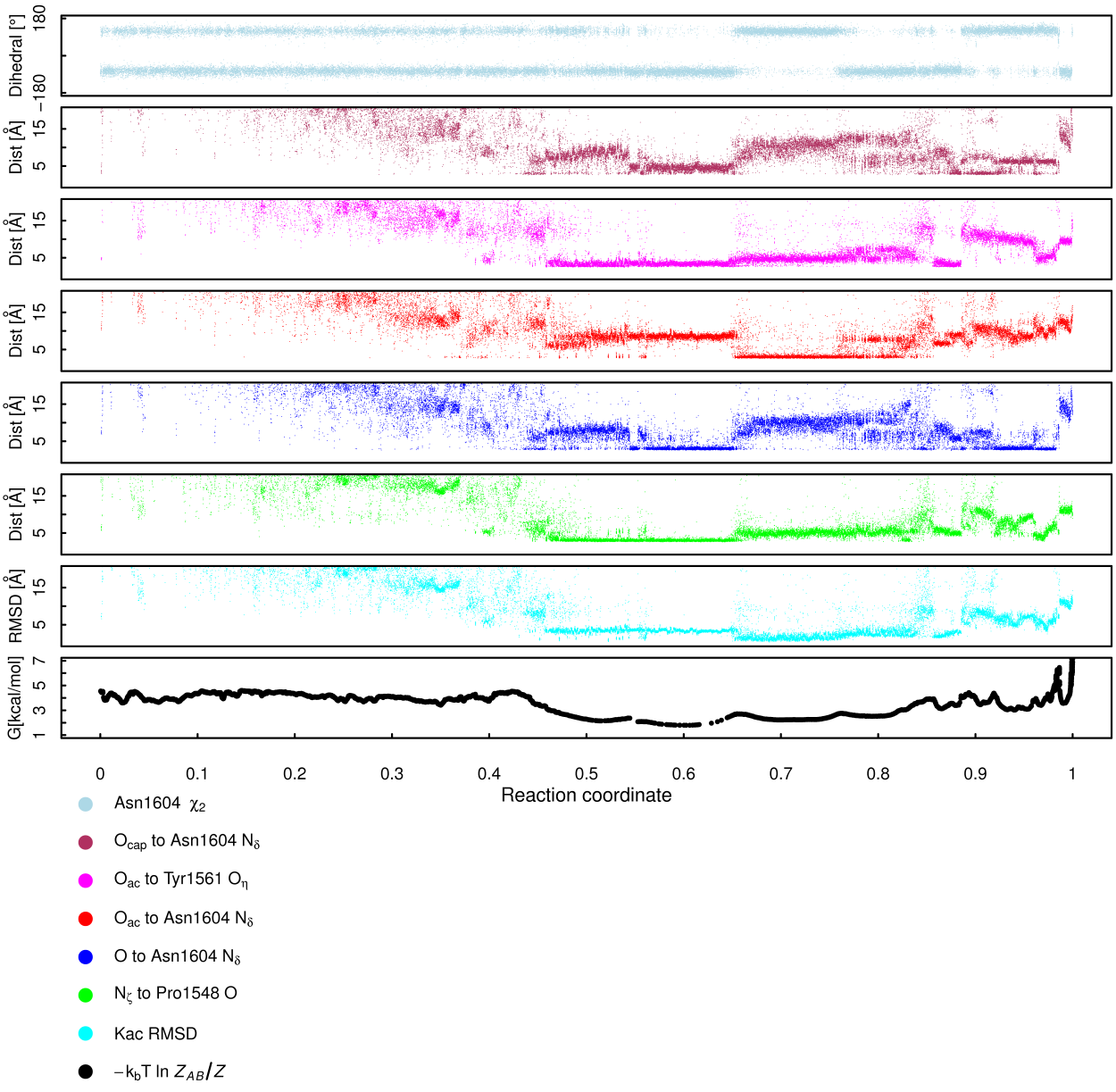

Figure S10: Geometric annotation and cFEP (bottom panel) from the unbound state. For further details see legend of Figure S7.